Structural Studies of Bicyclomycin

Harold Kohn [1], Syed Abuzar, and James D. Korp

Department of Chemistry, University of Houston,
Houston, TX 77004

Andrew S. Zektzer, and Gary E. Martin [1]

Department of Medicinal Chemistry, College of Pharmacy,
University of Houston, Houston, TX 77004

Received April 6, 1988

The complete ^1H and ^{13}C nmr assignments for both bicyclomycin (**1**) and bicyclomycin-3′-ethyl carbamate (**2**) were achieved through the combined use of a series of nmr techniques. Extensive use of the long range heteronuclear multiple quantum chemical shift correlation experiment (HMBC) permitted the assignments of all the exchangeable protons as well as the 2,5-piperazinedione carbonyl carbons in both compounds. The X-ray crystallographic structure of **2** was determined and compared to the reported structure of bicyclomycin. Compound **2** crystallizes in the orthorhombic space group $P2_12_12_1$ with four molecules in a unit cell having dimensions a = 7.931(2), b = 10.834(4), and c = 24.468(7) Å. The structure refined to a final R value of 6.2%.

J. Heterocyclic Chem., **25**, 1511 (1988).

Bicyclomycin (**1**) is a potent antibiotic of emerging importance for the treatment of nonspecific diarrhea in humans and bacterial diarrhea in calves and pigs [2]. Several intriguing scenarios have been proposed to account for the unusual pharmacological activity and chemical reactivity of this drug [3-6]. The pioneering studies of Iseki and co-workers demonstrated that bicyclomycin binds covalently with methyl mercaptan at the carbon-5 exomethylene unit at basic *p*Hs [3a]. This result coupled with other experiments led to the early hypothesis that the antibacterial activity of **1** is associated with the covalent binding of a sulfhydryl residue present on an inner-membrane protein to the terminal olefinic group of the drug [3]. New information concerning this critical reaction has been provided by ourselves [6] and the Williams' group [4b,c]. First, the structure of the bicyclomycin-methanethiolate adduct has been reassigned on the basis of detailed nmr studies [6]. Second, systematic variation of the substituents present in bicyclomycin and synthetic derivatives have suggested that both a free N10-H and a C1′-OH residue were necessary for thiolate addition to the exomethylene group [4b,c]. These findings have prompted new questions concerning the mechanism of this important transformation. Recently, Vasquez and co-workers have noted the close structural correspondence of **1** to the projected structure of the diaminopimelic acid-diaminopimelic acid unit within the peptidoglycan assembly of cellular membranes [5]. This similarity has raised the possibility that the drug functions as a competitive substrate for a protease involved in the biosynthesis of the bacterial cell envelope by reaction with an enzyme at one of the two ring carbonyl groups.

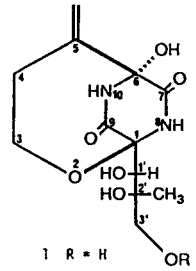

1 R = H

2 R = C(O)NHCH$_2$CH$_3$

Surprisingly, in light of these reports, few structural studies of bicyclomycin have appeared. The X-ray crystallographic analysis of **1** in 1974 has served as the major source of structural information to date concerning the drug [7]. In order to provide a basis set of data for future discussions on the interdependence of structure on the mode of action and chemical reactivity of bicyclomycin and the interaction of the drug with the peptidoglycan assembly during bacterial cell wall synthesis, we have undertaken a detailed nmr assignment of bicylcomycin and the corresponding 3′-ethyl carbamate derivative **2** [8]. Emphasis has been placed on assigning all the resonances for the exchangeable protons in the ^1H nmr spectra of **1** and **2**. Signals for the two piperazinedione carbonyl carbon resonances and the aminal resonances of the ^{13}C nmr spectra of **1** and **2** have also been unequivocally assigned. In addition, the X-ray crystallographic structure of **2** has been determined and compared to the reported structure of bicyclomycin (**1**) [7].

Results and Discussion.

a. NMR Studies.

The majority of the signals in the proton nmr spectra of bicyclomycin (**1**) and bicyclomycin-3′-ethyl carbamate (**2**) were readily assigned on the basis of chemical shift considerations and spin coupling patterns from the COSY

spectrum. The exchangeable proton assignments were less straightforward. In **1** tentative assignments were made for the C1′-OH proton as the doublet at 5.27 ppm, the C6-OH proton as the sharp singlet resonance at 6.83 ppm, and the C2′-OH as the sharp singlet at 4.48 ppm. In **2** the corresponding signals were tentatively ascribed to the peaks located at 5.51, 6.86, and 5.85 ppm, respectively. Initially the two amide protons in **1** resonating at 8.68 and 8.95 ppm, and in **2** appearing at 8.72 and 8.77 ppm, could not be unequivocally differentiated.

Table 1

Proton and Carbon NMR Chemical Shift Assignments for Bicyclomycin (**1**) and Bicyclomycin-3′-ethyl carbamate (**2**)

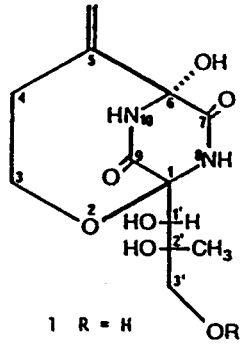

1 R = H

2 R = C(O)NHCH2CH3 (4′, 5′ 6′, 7′)

1 **2**

position	^{1}H	^{13}C	^{1}H	^{13}C
1	—	87.74	—	87.91
3	3.61, 3.80	63.27	3.61, 3.76	63.36
4	2.48	35.33	2.46	35.24
5	—	149.06	—	148.94
5a	5.04, 5.35	115.20	5.04, 5.36	115.19
6-OH	6.83	—	6.86	—
6	—	81.48	—	81.34
7	—	169.53	—	169.37
8-NH	8.68	—	8.72	—
9	—	166.25	—	165.96
10-NH	8.95	—	8.77	—
1′	3.89	70.47	3.87	69.54
1′-OH	5.27	—	5.51	—
2′	—	77.01	—	75.97
2′-CH_3	1.16	23.94	1.18	23.59
2′-OH	4.48	—	5.85	—
3′	3.33, 3.44	66.62	3.91, 3.99	68.50
3′-OH	5.21	—	—	—
4′	—	—	—	158.08
5′-NH	—	—	7.04	—
6′	—	—	2.98	34.92
7′	—	—	0.99	15.00

Given the proton resonance assignments contained in Table 1, a direct proton-carbon heteronuclear chemical shift correlation spectrum using the method described by Bax [9] with a BIRD pulse [10] incorporated midway through the evolution time to provide selective broadband vicinal proton decoupling gave the protonated carbon resonance assignments. Having completed the protonated carbon resonance assignments for **1** and **2** (see Table 1) there remained the task of assigning the non-protonated carbon resonances. A variety of methods are available for this purpose. Choices now exist between both proton and carbon detected variants of the long range heteronuclear correlation experiment. While the former has advantages in sensitivity, it is a more difficult experiment to perform and requires, at a minimum, access to a spectrometer with X-band pulse capabilities. Despite advantages in sensitivity, the proton detected long range heteronuclear multiple quantum correlation experiment (HMBC) described by Bax and Summers [11] is not applicable for the assignments of non-protonated carbon resonances in every case. Indeed, there may be instances when it is preferable to perform the heteronucleus detected experiment if sufficiently large samples of material are available. Specifically, problems arise in the digitization of the second frequency domain of the HMBC experiment (^{13}C). To provide adequate digitization in the second frequency domain, very substantial numbers of experiments must be performed, particularly when data are to be acquired for both carbonyl and aliphatic carbon resonances. At very high fields, *e.g.* 500 MHz, it may even be necessary to split the ^{13}C frequency range into two segments to provide adequate digital resolution and/or sufficiently effective pulse excitation [11].

For the assignment of bicyclomycin (**1**) both proton and carbon detected long range correlation experiments were employed. Each had distinct advantages. Only the proton detected (HMBC) long range spectrum, however, is shown in Figure 1. Key long range proton-carbon connectivity pathways for **1** are presented in Figure 2. Correlation pathways derived from the proton and carbon detected spectra were largely comparable. Initially, there was some difficulty in establishing the identities of the amide protons from the proton detected spectrum as there was no simple way to determine whether two bond ($^2J_{CH}$, *e.g.* H8 to C7 and H10 to C9) or three bond ($^3J_{CH}$, *e.g.* H8 to C9 and H10 to C7) coupling pathways would be favored when the experiment was optimized for an average 8 Hz long range coupling. This problem is solved, however, by a three bond coupling between one of the amide protons and the C5 vinyl carbon observed in the ^{13}C detected long range correlation experiment optimized for 10 Hz. Under these conditions, it is highly improbable that H8 would exhibit a long range coupling to C5 *via* a $^4J_{CH}$ coupling pathway. Hence, H10 was assigned as the amide proton

resonating at 8.95 ppm while H8 was assigned to the resonance at 8.68 ppm. Analysis of the remaining proton-carbon connectivities in the long range heteronuclear correlation experiments for **1** and **2** permitted the complete assignment of the signals in the nmr spectra of both compounds.

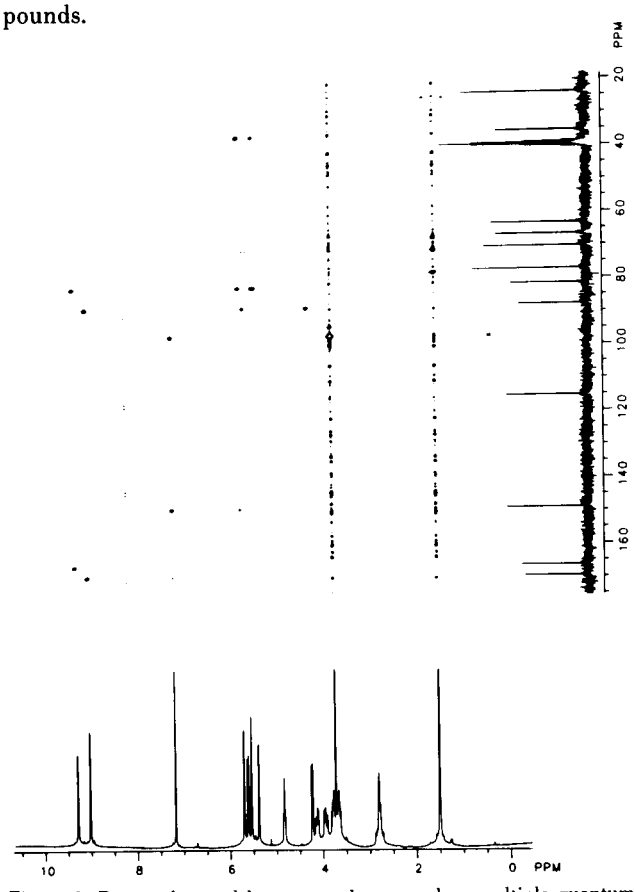

Figure 1. Proton detected long range heteronuclear multiple quantum chemical shift correlation (HMBC) nmr spectrum for **1**.

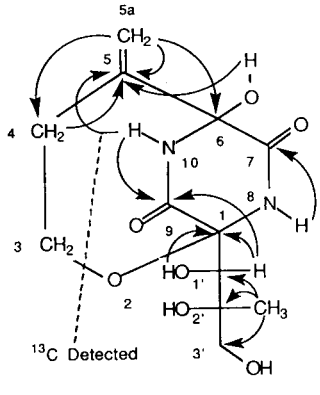

Figure 2. Long range proton carbon connectivities observed in the proton detected long range heteronuclear multiple quantum chemical shift correlation (HMBC) experiment for **1**. Arrows denote observed connectivities and emanate from the proton and terminate at the carbon which exhibited the response. One long range connectivity contained in the carbon detected spectrum is critical to the successful differentiation of the carbonyl and amide proton resonance assignments and is specifically noted in the figure.

b. X-ray Crystallographic Studies.

The nmr chemical shift values obtained for bicyclomycin-3′-ethyl carbamate (**2**) closely matched those observed for **1**. Verification of this structural correspondence in the solid was secured by determining the single-crystal structure of **2**. Figure 3 shows the atom labeling scheme based on the atomic coordinates given in Table 2. For the sake of continuity, the same numbering system was used as reported in the crystallographic analysis of **1** [7]. Tables 3 and 4 list the bond distances and angles for the non-hydrogen atoms. The agreement between the derived solid-state structures of **1** and **2** is remarkably good, especially considering that **1** was analyzed from film data and **2** contained disordered solvent and exhibited severe decay. In fact, none of the equivalent bond distances differs by more than 0.02 Å. A least squares fit of **1** and **2** is presented in Figure 4, showing the only major difference to be the orientation of O19. In **1** the O19 group is rotated so as to permit hydrogen bonding to O5, whereas in **2** O19 adopts an entirely different orientation in order to facilitate H-bonding between O16 and O23. For purposes of comparison we have inverted the listed coordinates [7] of **1** in order to conform to the absolute configuration determined some four years later [12].

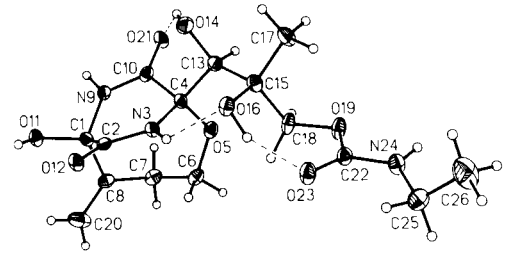

Figure 3. View of **2** showing the atom labeling. The nonhydrogen atoms are shown as 20% equiprobability ellipsoids, and hydrogens as spheres of arbitrary diameter. Intramolecular hydrogen bonds are indicated by dashed lines.

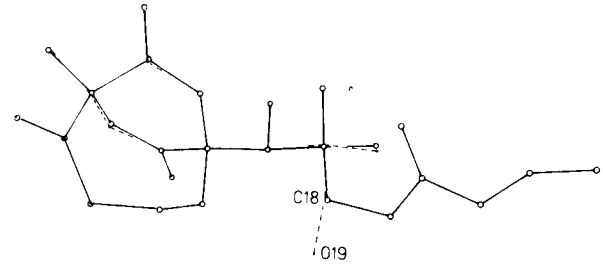

Figure 4. Least squares fit between inverted **1** (black dots) and **2** (open circles). Maximum deviation between equivalent atoms (excluding O19) is 0.2 Å.

Table 2

Atomic Coordinates ($\times 10^4$) and Equivalent Isotropic Displacement Parameters ($Å^2 \times 10^3$) for Bicyclomycin-3'-ethyl Carbamate (**2**)

	X	Y	Z	U(eq)
C(1)	8636(10)	6966(6)	7916(3)	37(2)
C(2)	7924(9)	6082(5)	7471(3)	34(2)
N(3)	6590(8)	6533(4)	7192(2)	36(1)
C(4)	6055(9)	7827(5)	7183(3)	39(2)
O(5)	4682(7)	8096(4)	7538(2)	47(1)
C(6)	4546(10)	7443(6)	8046(3)	49(2)
C(7)	5968(9)	7734(6)	8453(3)	50(2)
C(8)	7499(10)	6918(6)	8420(3)	44(2)
N(9)	8709(8)	8224(5)	7678(2)	38(1)
C(10)	7540(11)	8696(5)	7350(3)	43(2)
O(11)	10297(7)	6626(4)	8044(2)	44(1)
O(12)	8501(6)	5065(3)	7416(2)	46(1)
C(13)	5439(10)	8175(6)	6611(3)	43(2)
O(14)	6846(7)	8120(4)	6243(2)	56(1)
C(15)	3984(10)	7403(6)	6361(3)	45(2)
O(16)	4614(7)	6152(4)	6310(2)	46(1)
C(17)	3616(11)	7879(7)	5778(3)	61(2)
C(18)	2394(10)	7418(6)	6728(3)	49(2)
O(19)	844(6)	7200(4)	6433(2)	53(1)
C(20)	7870(13)	6104(7)	8807(3)	82(2)
O(21)	7532(8)	9778(3)	7197(2)	59(1)
C(22)	520(10)	6020(7)	6288(3)	44(2)
O(23)	1503(7)	5159(4)	6340(2)	62(1)
N(24)	−1044(8)	5931(5)	6087(3)	52(2)
C(25)	−1788(11)	4725(6)	5927(3)	63(2)
C(26)	−2602(16)	4775(8)	5399(3)	107(2)
O(27)	2351(10)	5557(5)	8982(3)	96(2)
C(28)	1857	6143	9472	96(2)
C(29)	2854	5712	9962	96(2)
O(27')	2902(26)	5853(19)	8966(10)	96(2)
C(28')	1567	5110	9164	96(2)
C(29')	1554	5000	9779	96(2)

* Equivalent isotropic U defined as one third of the trace of the orthogonalized U_{ij} tensor.

Examination of the crystallographic data revealed several interesting features. First, bonds C2-N3 and C10-N9 are considerably shorter than expected for a C-N single bond, whereas C1-C2 and C4-C10 are somewhat longer than anticipated for bonds involving an sp^2 hybridized atom. These results indicate that there exists significant double bond character in the C-N part of the peptide linkage. Comparable observations have been noted in related compounds [13]. The fact that the N and O atoms are in-

Table 3

Bond Lengths (Å) for Bicyclomycin-3'-ethyl Carbamate (**2**)

C(1)-C(2)	1.553 (8)	C(1)-C(8)	1.527 (9)
C(1)-N(9)	1.480 (7)	C(1)-O(11)	1.400 (8)
C(2)-N(3)	1.348 (8)	C(2)-O(12)	1.196 (7)
N(3)-C(4)	1.460 (7)	C(4)-O(5)	1.421 (8)
C(4)-C(10)	1.558 (9)	C(4)-C(13)	1.527 (8)
O(5)-C(6)	1.433 (7)	C(6)-C(7)	1.535 (9)
C(7)-C(8)	1.500 (10)	C(8)-C(20)	1.326 (9)
N(9)-C(10)	1.326 (8)	C(10)-O(21)	1.227 (6)
C(13)-O(14)	1.434 (8)	C(13)-C(15)	1.547 (10)
C(15)-O(16)	1.446 (7)	C(15)-C(17)	1.546 (9)
C(15)-C(18)	1.545 (10)	C(18)-O(19)	1.443 (8)
O(19)-C(22)	1.347 (8)	C(22)-O(23)	1.218 (8)
C(22)-N(24)	1.336 (9)	N(24)-C(25)	1.481 (9)
C(25)-C(26)	1.445 (10)	O(27)-C(28)	1.412
O(27)-O(27')	0.542 (22)	C(28)-C(29)	1.508
C(28)-C(28')	1.366 (23)	C(29)-C(29')	1.361 (22)
O(27')-C(28')	1.412	C(28')-C(29')	1.508

Table 4

Bond Angles (°) for Bicyclomycin-3'-ethyl Carbamate (**2**)

C(8)-C(1)-C(2)	109.4(6)	N(9)-C(1)-C(2)	107.6(5)
N(9)-C(1)-C(8)	111.8(5)	O(11)-C(1)-C(2)	109.6(5)
O(11)-C(1)-C(8)	111.3(5)	O(11)-C(1)-N(9)	107.0(6)
N(3)-C(2)-C(1)	114.6(5)	O(12)-C(2)-C(1)	120.3(6)
O(12)-C(2)-N(3)	125.0(6)	C(4)-N(3)-C(2)	125.5(6)
O(5)-C(4)-N(3)	114.1(6)	C(10)-C(4)-N(3)	110.7(6)
C(10)-C(4)-O(5)	107.0(5)	C(13)-C(4)-N(3)	110.1(5)
C(13)-C(4)-O(5)	105.4(6)	C(13)-C(4)-C(10)	109.4(5)
C(6)-O(5)-C(4)	119.2(5)	C(7)-C(6)-O(5)	114.0(6)
C(8)-C(7)-C(6)	115.9(5)	C(7)-C(8)-C(1)	120.0(6)
C(20)-C(8)-C(1)	118.0(8)	C(20)-C(8)-C(7)	121.9(7)
C(10)-N(9)-C(1)	124.3(6)	N(9)-C(10)-C(4)	117.0(5)
O(21)-C(10)-C(4)	119.3(7)	O(21)-C(10)-N(9)	123.6(7)
O(14)-C(13)-C(4)	108.5(6)	C(15)-C(13)-C(4)	117.8(6)
C(15)-C(13)-O(14)	107.9(5)	O(16)-C(15)-C(13)	106.3(6)
C(17)-C(15)-C(13)	109.1(6)	C(17)-C(15)-O(16)	107.2(6)
C(18)-C(15)-C(13)	111.8(6)	C(18)-C(15)-O(16)	109.9(6)
C(18)-C(15)-C(17)	112.3(6)	O(19)-C(18)-C(15)	113.5(5)
C(22)-O(19)-C(18)	116.6(6)	O(23)-C(22)-O(19)	124.9(7)
N(24)-C(22)-O(19)	109.9(7)	N(24)-C(22)-O(23)	125.1(7)
C(25)-N(24)-C(22)	121.9(6)	C(26)-C(25)-N(24)	112.4(7)
C(29)-C(28)-O(27)	113.1	C(29')-C(28')-O(27')	113.1

volved in hydrogen bonding probably does not contribute appreciably to the N-C-O resonance, since other compounds having no such H-bonding display similar geometry [14]. All remaining bond lengths in **2** are as expected, in excellent agreement with literature values. Second, the piperazinedione ring in **2** adopted a twist-boat conformation. 2,5-Piperazinediones are ubiquitous in nature [15], and a large number of X-ray structures containing this group have been reported. Several conformations have been observed, ranging from chair to planar to boat. Factors which affect the adopted conformation include degree of amide resonance, steric repulsions between C1 and C4 substituents, hydrophobic interactions between ring substituents and hydrogen bonding. Although Tokuma and co-workers described the ring system of **1** as a boat [7], it would be more accurately viewed as a twist-boat, since the C2/N3/C10/N9 atoms are somewhat skewed rather than strictly planar. The same distortion is found in the piperazinedione ring of **2**, as evident from comparison of torsion angles (C1-C2-N3-C4 = 15.4° *vs.* C1-N9-C10-C4 = −3.7°). This distortion makes it very difficult to measure the fold angle of the ring along the C1-C4 vector, however the best values obtained (145° for **1** and 143° for **2**) are considerably flatter than noted in some other analogues (130° to 134°). Significantly, the boat configuration is not restricted solely to bicylic compounds, since this conformation has also been noted in cases where no bridge exists between C1 and C4 [18]. This analysis suggests there is no undue strain inherent in the fused ring system itself. Third, although the long side chain at C4 has an almost completely flexible backbone, intramolecular hydrogen bonds involving O16 virtually lock it into a rigid conformation in the solid state, much as in bicyclomycin itself (see Figure 3). There is also an extensive intermolecular hydrogen bonding system, which is shown in Figure 5 and summarized in Table 5. As is typically observed, the O-H···O bonds are stronger than the N-H···O types [19], with the exception of O14···O21 which is geometrically constrained and may in fact not be a true hydrogen bond. If it is a hydrogen bond, then it is bifurcated, since H14 also points in the direction of O27. The intermolecular bonds form the molecules into thick sheets parallel to the *ab* plane, interspersed by layers of ethanol. The hydrogen bonding parameters are in good agreement with those found in other piperazinediones [13b,c].

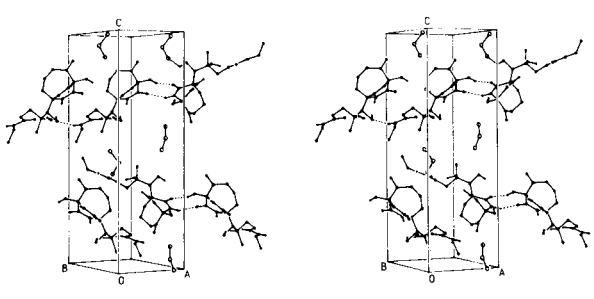

Figure 5. Stereoscopic view of the packing in the unit cell **2**. Intermolecular hydrogen bonds are shown as dashed lines.

Table 5

Hydrogen Bonding Parameters for Bicyclomycin-3′-ethyl Carbamate (**2**)

A-B···C	A-B	A···C	B···C	< B
Intramolecular:				
N(3),H(3),O(16)	0.95	2.70	2.00	129
O(16),H(16),O(23)	0.95	2.69	1.80	155
O(14),H(14),O(21)	0.95	2.99	2.18	142
Intermolecular:				
N(9),H(9),O(12)	0.95	2.98	2.10	154
O(11),H(11),O(21)	0.95	2.70	1.86	146
N(24),H(24),O(14)	0.88	2.92	2.08	159
O(14),H(14),O(27)	0.95	2.77	2.10	126

Conclusions.

The complete ^1H and ^{13}C nmr assignments of bicyclomycin (**1**) and bicyclomycin-3′-ethyl carbamate (**2**) have been determined using a battery of nmr techniques. Of particular importance was the application of the long range heteronuclear multiple quantum chemical shift correlation experiment (HMBC) recently described by Bax and Summers [11]. This procedure permitted the unequivocal assignment of the ring amide protons, the ring aminal and carbonyl carbons, as well as the remaining exchangeable protons in the molecule. The availability of unequivocal assignments for all of the resonances in the proton and carbon nmr spectra of **1** in particular is important for several reasons. In part, these assignments may ultimately facilitate nmr studies of the potential interactions of this novel antibiotic with the peptidoglycan assembly during bacterial cell wall synthesis in light of current notions concerning the mode of action of the drug [3-6]. More immediately, these assignments have proven crucial in establishing the identity [6] of the addition product produced when bicyclomycin is treated with sodium methanethiolate under basic conditions [3a].

EXPERIMENTAL

NMR Studies.

All of the nmr spectra were recorded using a Nicolet NT-300 wide bore spectrometer equipped with a 5 mm $^1H/^{13}C$ dual tuned probe and controlled by a Model 293-C pulse programmer. Observation frequencies for ^1H and ^{13}C were 300.042 and 75.455 MHz, respectively. The 90° observe pulse widths were 13.8 and 18.3 μsec for ^1H and ^{13}C, respectively; the 90° pulse from the decoupler coils was 32.2 μsec and was calibrated using the pulsed method of Bax [20].

The spectrometer was extensively modified for proton detected long range heteronuclear multiple quantum experiments using the pulse sequence described by Bax and Summers [11,21]. The proton decoupler was used as a 300 MHz frequency source which was mixed with 225 MHz generated by doubling the 112.5 MHz output of a Fluke 160 frequency synthesizer. The output was filtered to remove the 525 MHz component leaving the required 75 MHz frequency. The final 75 MHz output was amplified by a narrowband class C amplifier to generate the desired 80 W ^{13}C pulse from the decoupler. The 90° ^{13}C "decoupler" pulse obtained from the modifications just described was calibrated as 12 μsec using at 30% w/v solution of 99% enriched 2-^{13}C-sodium acetate in deuterium oxide using the pulsed calibration method [20].

Autocorrelated Proton (COSY) Chemical Shift Correlation Experiments.

Proton-proton homonuclear chemical shift correlations were established using the COSY experiment [22]. A 16 step phase cycle was employed and the data were taken as 256 × 512 complex points (2 hours). The data were processed using sinusoidal multiplication prior to both Fourier transformations and were symmetrized [23] prior to plotting.

Direct ($^1J_{CH}$) Heteronuclear Chemical Shift Correlation Experiments.

Direct heteronuclear correlations were established using the basic heteronuclear correlation sequence [24,25] modified to provide semi-selective vicinal homonuclear proton decoupling by the inclusion of a BIRD pulse midway through the evolution period as described by Bax [9]. Spectra were acquired on samples containing either 75 mg of **1** or 30 mg of **2** which were dissolved in 0.4 mℓ of 100% DMSO-d_6. Data were taken as 128 × 1K complex points (overnight) and were processed using exponential apodization prior to the first Fourier transformation and zero filling to 256 points and double exponential apodization prior to the second Fourier transform to give a final data matrix consisting of 256 × 512 points.

Long range ($^nJ_{CH}$, n = 2,3) Heteronuclear Chemical Shift Correlation Experiments.

a. ^{13}C Detection.

Long range heteronuclear chemical shift correlation using heteronucleus (^{13}C) detection was performed using the pulse sequence recently reported by Zektzer, John and Martin [26] which incorporated a BIRD pulse midway through the Δ_2 refocusing interval to suppress one bond modulation of protonated carbon long range responses. The experiment was performed using the sample of **1** containing 75 mg in 0.4 mℓ of 100% DMSO-d_6. The data were acquired as 128 × 1K complex points (overnight) and were processed as above.

b. ^1H Detection.

Long range proton-carbon heteronuclear correlations were also established *via* ^1H detection using the pulse sequence described by Bax and Summers [11,21]. The data were acquired using a sample containing either 30 mg of **1** or **2** dissolved in 0.4 mℓ of 100% DMSO-d_6. The eight step phase cycle according to Bax and Summers [11] was expanded to 32 steps by superimposition of a cyclops cycle over the existing eight step cycle. Prior to accumulation, 4 dummy scans were taken and discarded for each evolution time. Proton T_1 relaxation times were measured and the experiment was cycled as a function of 2 × T_1 = 1.7 sec. The initial data matrix consisted of 425 × 1K complex points (24 hours) and the sample was not spun to reduce t_1 noise. The data were processed using sinusoidal multiplication and exponential multiplication prior to the first Fourier transformation. The data matrix was zero filled to 512 points and subjected to exponential multiplication prior to the second Fourier transformation to afford a final data matrix comprised of 512 × 512 points.

X-ray Crystallographic Study of **2**.

Bicyclomycin-3'-ethyl carbamate (**2**) was recrystallized from ethanol. A large clear colorless fragment of **2** having approximate dimensions 0.60 × 0.40 × 0.13 mm was cut from a very large plate and mounted on a glass fiber in a random orientation on a Nicolet R3m/V automatic diffractometer. The radiation used was Mo Kα monochromatized by a highly ordered graphite crystal. Final cell constants, as well as other information pertinent to data collection and refinement, are listed in Table 6. The Laue symmetry was determined to be mmm, and from the systematic absences noted the space group was shown unambiguously to be $P2_12_12_1$. Sample peak profiles run on certain reflections in order to ascertain optimum scan width showed occasional asymmetry, and this was assumed to be due to minor crystal damage during handling. A slightly wider than normal scan width was used in order to ensure uniform backgrounds. Intensities were measured using the omega scan technique, with the scan rate depending on the count obtained in rapid pre-scans of each reflection. Two standard reflections were monitored after every two hours or every 100 data collected, and these showed rapid, linear decay amounting to over 60% by the end of the 48 hours of the experiment. A normalizing factor as a function of exposure time was used to account for this. In reducing the data, Lorentz and polarization corrections were applied, however no correction for absorption was made due to the small absorption coefficient.

Table 6

Data Collection and Processing Parameters for Bicyclomycin-3'-ethyl Carbamate (**2**)

Space group	$P2_12_12_1$ (orthorhombic)
Cell constants	a = 7.931(2)Å b = 10.834(4) c = 24.468(7) V = 2102Å^3
Molecular formula	$C_{15}H_{23}N_3O_8 \cdot C_2H_6O$
Formula weight	419.5
Formula units per cell	Z = 4
Density	ρ = 1.33 g-cm^{-3}
Absorption coefficient	μ = 1.01 cm^{-1}
Radiation (Mo Kα)	λ = 0.71073Å
Collection range	$4° \leq 2\theta \leq 55°$
Scan width	$\Delta\theta = 1.2 + (K\alpha_2\text{-}K\alpha_1)°$
Scan speed range	1.5 to 15.0° −min^{-1}
Total data collected	2759
Independent data, $I > 3\sigma(I)$	1598
Total variables	271
$R = \Sigma\|\|F_o\|-\|F_c\|\|/\Sigma\|F_o\|$	0.062
$R_w = [\Sigma w(\|\|F_o\|-\|F_c\|)^2/\Sigma w\|F_o\|^2]^{1/2}$	0.049
Weights	$w = \sigma(F)^{-2}$

The solution of the structure was obtained from TREF using SHELXTL PLUS direct methods, yielding coordinates for all non-solvent atoms in the asymmetric unit. The usual sequence of isotropic and anisotropic refinement was followed, after which all hydrogens were entered in ideal calculated positions. Only the positions of H3, H9, H11, H14, H16, and H24 were allowed to refine independently, and reasonable distance constraints were applied in order to facilitate refinement. A single isotropic thermal parameter was refined for all of the hydrogen atoms. At this point, a difference Fourier synthesis revealed the position of a heavily disordered solvent molecule, which is presumed to be ethanol. The atoms involved refined poorly, and eventually had to be treated as rigid bodies based on bonding geometry found in the initial difference map. Two distinct orientations of the ethanol were noted, and when the population factors were allowed to vary they refined to 80%:20% for the O27:O27' sites. In the final cycles of least squares the occupancies were thus fixed at 0.80 and 0.20 while a single isotropic thermal parameter for

all solvent atoms was varied. Hydrogens were added at ideal calculated positions with appropriate occupancies.

An extensive hydrogen bonding system is present, as indicated in Table 5. H14 appears to be involved in a bifurcated bonding arrangement with O21 and O27, but this may be due to slight mispositioning of H14 during refinement. Unfortunately the heavy disorder of the ethanol solvent molecule prevented location of H27, but examination of the packing diagram reveals that the missing hydrogen would probably be involved in a weak attraction to O11. The calculated separation between O11 and O27 is approximately 3.0Å. There are no heavy atoms in the compound and thus it is impossible to determine experimentally the correct absolute configuration. Therefore the chirality was adjusted in order to match that determined for bicyclomycin by analysis of an acid-catalyzed rearrangement product [12]. After all shift/esd ratios were less than 0.1, convergence was reached at the agreement factors listed in Table 6. No unusually high correlations were noted between any of the variables in the last cycle in full-matrix least squares refinement, and the final difference density map showed no peaks greater than 0.30 e/A^3. All calculations were made using Nicolet's SHELXTL PLUS (1987) series of crystallographic programs.

Acknowledgements.

We thank the National Institutes of Health (GM 37934) and the Robert A. Welch Foundation (H.K., E-607; G. E. M., E-792) for their generous support of this research. The National Science Foundation (CHE-8616352) is gratefully acknowledged for providing matching funds for the purchase of one of the nmr spectrometers used in this study. We also express our appreciation to Dr. K. Inokuchi and the Fujisawa Pharmaceutical Co., Ltd., Japan for providing us with a gift of bicyclomycin.

Supplementary Material.

Anisotropic Displacement Parameters (Table 7), H-Atom Coordinates and Isotropic Displacement Parameters (Table 8), Torsion Angles (Table 9), and the Observed and Calculated Structure Factors (Table 10) for compound **2** (9 pages) are available from the authors.

REFERENCES AND NOTES

[1] To whom inquiries should be addressed.

[2a] N. Tanaka, *Antibiotics (N.Y.)*, **5**, 18 (1979); [b] T. Miyoshi, N. Miyari, H. Aoki, M. Kohsaka, H. Sakai and H. Imanaka, *J. Antibiot.*, **25**, 569 (1972); [c] T. Kamiya, S. Maeno, M. Hashimoto, and Y. Mine, *ibid.*, **25**, 576 (1972); [d] M. Nishida, Y. Mine, and T. Matsubara, *ibid.*, **25**, 582 (1972); [e] M. Nishida, Y. Mine, T. Matsubara, S. Goto, and S. Kuwahara, *ibid.*, **25**, 594 (1972).

[3a] A. Someya, M. Iseki, and N. Tanaka, *J. Antibiot.*, **32**, 402 (1972); [b] N. Tanaka, M. Iseki, T. Miyoshi, H. Aoki, and H. Imanaka, *ibid.*, **29**, 155 (1976); [c] A. Someya, M. Iseki, and N. Tanaka, *ibid.*, **31**, 712 (1978).

[4a] R. M. Williams, R. W. Armstrong, and J.-S. Dung, *J. Med. Chem.*, **28**, 733 (1985); [b] R. M. Williams, K. Tomizawa, R. W. Armstrong, and J.-S. Dung, *J. Am. Chem. Soc.*, **107**, 6419 (1985); [c] R. M. Williams, K. Tomizawa, R. W. Armstrong, and J.-S. Dung, *ibid.*, **109**, 4028 (1987).

[5] A. G. Pisabarro, F. J. Canada, D. Vasquez, P. Arriaga, and A. J. Rodriguez-Tebar, *J. Antibiot.*, **34**, 914 (1986).

[6] H. Kohn and S. Abuzar, *J. Am. Chem. Soc.*, **110**, 3661 (1988).

[7] Y. Tokuma, S. Koda, T. Miyoshi, and Y. Morimoto, *Bull. Chem. Soc. Japan*, **47**, 18 (1974).

[8] B. W. Muller, O. Zak, W. Kump, W. Tosch, and O. Wacker, *J. Antibiot.*, **32**, 689 (1979).

[9] A. Bax, *J. Magn. Reson.*, **53**, 517 (1983).

[10] J. R. Garbow, D. P. Weitekamp, and A. Pines, *Chem. Phys. Letters*, **93**, 504 (1982).

[11] A. Bax and M. F. Summers, *J. Am. Chem. Soc.*, **108**, 2093 (1986).

[12] For the absolute configuration of bicyclomycin, see: H. Maag, J. F. Blount, D. L. Coffen, T. V. Steppe, and F. Wong, *J. Am. Chem. Soc.*, **100**, 6786 (1978).

[13a] H. Seya, K. Nozawa, S. Nakajima, K. Kawai, and S. Udagawa, *J. Chem. Soc., Perkin Trans. I*, 109 (1986); [b] C. Howes, N. W. Alcock, B. T. Golding, and R. W. McCabe, *J. Chem. Soc., Perkin Trans. I*, 2287 (1983); [c] F. Mazza, G. Lucente, F. Pinnen, and G. Zanotti, *Acta Cryst.*, **C40**, 1974 (1984).

[14] J. D. Korp and I. Bernal, *J. Cryst. Spect. Res.*, **15**, 181 (1985).

[15] P. G. Sammes, *Fortschr. Chem. Org. Naturst.*, **32**, 51 (1975).

[16] H. C. J. Ottenheijm, R. Plate, J. H. Noordik, and J. D. M. Herscheid, *J. Org. Chem.*, **47**, 2147 (1982).

[17] J. Fridrichsons and A. McL. Mathieson, *Acta Cryst.*, **18**, 1043 (1965).

[18] R. M. Williams, O. P. Anderson, R. W. Armstrong, J. Josey, H. Meyers and C. Erikson, *J. Am. Chem. Soc.*, **104**, 6092 (1982).

[19a] A. Whuler, C. Brouty, and P. Spinat, *Acta. Cryst.*, **B36**, 1267 (1980); [b] S. C. Wallwork, *Acta Cryst.*, **15**, 758 (1962).

[20] A. Bax, *J. Magn. Reson.*, **52**, 76 (1983).

[21] For additional information, see: A. S. Zektzer, L. D. Sims, R. N. Castle, and G. E. Martin, *Magn. Reson. Chem.*, **26**, 287 (1988).

[22] A. Bax, R. Freeman, and G. A. Morris, *J. Magn. Reson.*, **42**, 164 (1981).

[23] R. Baumann, G. Wider, R. R. Ernst, and K. Wuthrich, *J. Magn. Reson.*, **44**, 402 (1981).

[24] R. Freeman and G. A. Morris, *J. Chem. Soc., Chem. Commun.*, 684 (1978).

[25] A. Bax and G. A. Morris, *J. Magn. Reson.*, **42**, 501 (1981).

[26] A. S. Zektzer, B. K. John, and G. E. Martin, *Magn. Reson. Chem.*, **25**, 752 (1987).